



Comparison of Two Computational Microstructure Models for Predicting Effective Transverse Elastic Properties of Unidirectional Fiber Reinforced Composites

W. Lin^a, H. Wang^{*a,b}, Y. Zhang^a

^a College of Civil Engineering & Architecture, Henan University of Technology, Zhengzhou, China

^b State Key Laboratory of Structural Analysis for Industrial Equipment, Dalian University of Technology, Dalian, China

PAPER INFO

Paper history:

Received 10 November 2017

Received in revised form 23 December 2017

Accepted 04 January 2018

Keywords:

Fiber-reinforced Composite
Effective Transverse Elastic Properties
Free Boundary
Straight-edge Boundary
Finite Element

ABSTRACT

Characterization of properties of composites has attracted a great deal of attention towards exploring their applications in engineering. The purpose of this work is to study the difference of two computational microstructure models which are widely used for determining effective transverse elastic properties of unidirectional fiber reinforced composites. The first model based on the classic mechanics of materials permits free unloaded opposite boundaries in the unit cell; while the second one introduces straight-edge constraints in the unit cell to represent interactions of neighboring cells during deformation. The two approaches are firstly verified by the periodic circular hole problems. Then three microstructures are taken into consideration including the circular fibers, square fibers, and circular fiber clusters periodically embedded in the matrix and subsequently are solved by finite element analysis. A comparison of the numerical results demonstrated that the two computational models with and without periodic conditions can give different predictions on the effective elastic properties of composite for both low and high fiber volume fractions, especially for the effective Poisson's ratio of composite. Applying periodic straight-edge constraints after deformation can prevent any over-constrained conditions in the numerical model and give more stable results.

doi: 10.5829/ije.2018.31.09c.04

1. INTRODUCTION

Unidirectional fiber reinforced composites have been widely used in practical engineering situations due to their higher stiffness-to-weight and strength-to-weight ratio over those of single phase materials [1-5]. Such application requirements have made necessary the development of effective tools to predict their whole mechanical properties. With the assumption of periodicity of fiber arrangement in a matrix, homogenization process, that is an averaging of local properties, can be performed in a representative volume element, or a unit cell, which usually includes a single fiber surrounded by a matrix, so that the analytical cost is greatly reduced [6, 7]. The properties of composite as a whole are assumed to be same as those of this characteristic unit cell. Once a unit cell is cut from

periodic composite, the proper boundary constraints can be applied to its boundary, so that the unit cell can be further solved numerically by the finite element simulation [8-10], the boundary element method (BEM) [11, 12] or the hybrid finite element method [13-16], etc, to obtain stress and displacement variations in unit cell. These approaches are important to perform homogenization analysis for determining the overall properties of composite. Currently, there are several homogenization approaches available for determining effective elastic properties of such composite materials [17]. Actually, the longitudinal modulus of composite can be well predicted by the simplest rule of mixture, while the prediction of transverse elastic properties of composite is still on the way. Moreover, there is lack of a comparison of results from these predictive approaches to give more practical guidance to engineers.

In this paper, the comparison of two predictive approaches is made, including the mechanics of

* Corresponding author: huiwang@haut.edu.cn (H. Wang)

materials approach [12, 18, 19] and the eigenfunction expansion variational method [8, 11, 20], which are widely used as tools for predicting overall transverse elastic properties of composites. In the first predictive approach, the free boundary conditions on unloaded opposite edges of the unit cell are introduced. For the second approach, the periodic straight-edge constraints are applied along the whole boundary of the unit cell to represent the deformation constraint of neighboring cells in the whole composite. Correspondingly, the chosen unit cell is solved by finite element analysis to give the stress and displacement distributions, so that the effective elastic properties can be further obtained. In order to fully compare these two approaches, the effects of volume fraction of fibers, as well as the fiber shape and the fiber distribution are investigated. In addition to the regular distribution of fibers in the matrix, the influence of fiber cluster is also considered in this study.

2. MICROMECHANICAL COMPUTATIONAL MODELS

In this paper, the effective transverse mechanical properties of unidirectional fiber reinforced composites are determined by two different computational models. It is assumed that the general-shaped fibers are periodically dispersed in the matrix material in a square pattern. This means that a unit cell shown in Figure 1, can be taken from the composite for further analysis such that the effective properties of composite in a whole is same as those of the unit cell. For simplicity, it is assumed that both the fiber and the matrix are isotropic and homogeneous, and they are perfectly bonded on their common interface. Theoretically, the transverse plane of composite with arbitrarily shaped fibers can be considered to be homogeneous and anisotropic, thus the transverse constitutive relation under plane stress state can be written as follows:

$$\begin{aligned} \varepsilon_{11} &= \sigma_{11} / E_1 - \nu_{12} \sigma_{22} / E_2 \\ \varepsilon_{22} &= -\nu_{12} \sigma_{11} / E_1 + \sigma_{22} / E_2 \\ \gamma_{12} &= \tau_{12} / G_{12} \end{aligned} \quad (1)$$

where ε_{ij} ($i, j = 1, 2$) and σ_{ij} ($i, j = 1, 2$) are strain and stress components, E_i ($i = 1, 2$) denotes the Young's modulus in the direction x_i , ν_{ij} represents the Poisson's ratio of negative of the normal strain in the direction x_j to the normal strain in the direction x_i , and G_{12} denotes the shear modulus in the coordinate plane $x_1 - x_2$.

Additionally, the engineering constants in Equation (1) should satisfy the following reciprocal relation:

$$\nu_{12} / E_1 = \nu_{21} / E_2 \quad (2)$$

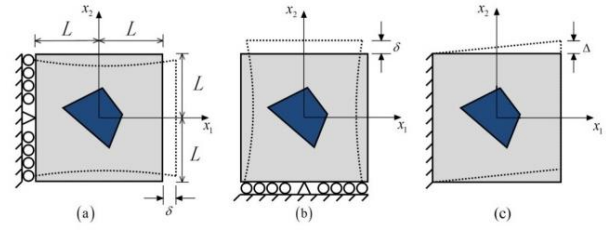


Figure 1. The unit cell under (a) uniform tension along the x_1 direction, (b) uniform tension along the x_2 direction and (c) in-plane shear

2. 1. Free Boundary Model For this computational model, which was widely employed for determining effective elastic properties of composites [1, 12, 18, 19, 21], three sets of boundary conditions are applied on the boundary of the unit cell, as shown in Figure 1.

Uniform tension

For the case of uniform tension along the x_1 direction, as illustrated in Figure 1(a), δ is the prescribed value of displacement.

The unit cell can be solved by the finite element simulations. Further, the average stress along the right edge of the unit cell can be evaluated by:

$$\bar{\sigma}_{11} = \left[\int_{-L}^L \sigma_{11}(L, x_2) dx_2 \right] / 2L \quad (3)$$

Correspondingly, the average normal strain along the x_1 direction and the x_2 direction can be given by:

$$\begin{aligned} \bar{\varepsilon}_{11} &= \delta / 2L \\ \bar{\varepsilon}_{22} &= \left[-\int_{-L}^L u_2(x_1, L) dx_1 + \int_{-L}^L u_2(x_1, -L) dx_1 \right] / 4L^2 \end{aligned} \quad (4)$$

where u_1 and u_2 are the displacements along the x_1 and x_2 directions, respectively. Then from the constitutive relation one obtains:

$$E_1 = \bar{\sigma}_{11} / \bar{\varepsilon}_{11}, \quad \nu_{12} = -\bar{\varepsilon}_{22} / \bar{\varepsilon}_{11} \quad (5)$$

Similarly, for the unit cell shown in Figure 1(b) under uniform tension along the x_2 direction, solving it can give the stress variations in it, then the average tensile stress along the upper edge is evaluated by:

$$\bar{\sigma}_{22} = \left[\int_{-L}^L \sigma_{22}(x_1, L) dx_1 \right] / 2L \quad (6)$$

Correspondingly, the average normal strain $\bar{\varepsilon}_{22} = \delta / 2L$. Then the effective Young's modulus along the x_2 direction can be given by:

$$E_2 = \bar{\sigma}_{22} / \bar{\varepsilon}_{22} \quad (7)$$

In-plane shear

For the in-plane shear case, as shown in Figure 1(c), Δ is the given value of displacement. Once the stress

variation in the unit cell is determined by finite element analysis, the effective shear modulus, the average shear stress $\bar{\tau}_{12}$ and the average shear strain $\bar{\gamma}_{12}$ in the transverse plane can be given by:

$$\bar{\tau}_{12} = \left[\int_{-L}^L \tau_{12}(L, x_2) dx_2 \right] / 2L, \quad \bar{\gamma}_{12} = \Delta / 2L \quad (8)$$

from which we have the effective shear modulus $G_{12} = \bar{\tau}_{12} / \bar{\gamma}_{12}$.

2. 2. Straight-side Model

To represent the constraint of neighboring cells to the one under study, the proper periodic straight edge condition should be taken into consideration. Applying periodic boundary conditions can prevent any over-constrained conditions in the numerical model and result in more accurate predictions of overall properties. Here, the computational model based on the eigenfunction expansion variational method [8, 22] is described by introducing periodic deformation in periodic composites. For simplicity, such computational model is called as straight-edge model. In this computational model, the suitable periodic boundary conditions are applied along the outer boundary of cell to keep the boundaries straight after the deformation. Figure 2 displays the cases of biaxial tension and shear deformation.

Biaxial tension

As shown in Figure 2(a), the the unict cell is subjected to the biaxial tension, and δ_1 and δ_2 are respectively the unknown displacements, which are set to keep the four edges of the unit cell straight after deformation.

When a constant stress p is applied along the x_1 direction, the equilibrium relationship of the unit cell can be written as follows:

$$\begin{aligned} \left[\int_{-L}^L \sigma_{11}^{(1)}(L, x_2) dx_2 \right] \delta_2 + \left[\int_{-L}^L \sigma_{11}^{(2)}(L, x_2) dx_2 \right] \delta_1 &= 2Lp \\ \left[\int_{-L}^L \sigma_{22}^{(1)}(x_1, L) dx_1 \right] \delta_2 + \left[\int_{-L}^L \sigma_{22}^{(2)}(x_1, L) dx_1 \right] \delta_1 &= 0 \end{aligned} \quad (9)$$

where $\sigma_{11}^{(1)}$ and $\sigma_{22}^{(1)}$ are stresses in the submodel 1, and $\sigma_{11}^{(2)}$ and $\sigma_{22}^{(2)}$ are stresses in the submodel 2, as indicated in [8, 11, 22]. Obviously, solving the linear system of equations, one can get δ_1 and δ_2 . Then the average strains can be given by:

$$\bar{\varepsilon}_{11} = \delta_1 / L, \quad \bar{\varepsilon}_{22} = \delta_2 / L, \quad \bar{\gamma}_{12} = 0 \quad (10)$$

Considering the constant stress state $\bar{\sigma}_{11} = p$, $\bar{\sigma}_{22} = 0$, $\bar{\sigma}_{12} = 0$. From the constitutive relation in Equation (1), one can determine the effective Young's modulus and Poisson's ratio of the composite by:

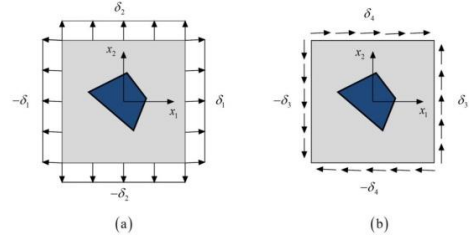


Figure 2. Unit cell under periodic boundary conditions for (a) biaxial tension and (b) in-plane shear

$$E_1 = \bar{\sigma}_{11} / \bar{\varepsilon}_{11} = pL / \delta_1, \quad \nu_{12} = -\bar{\varepsilon}_{22} / \bar{\varepsilon}_{11} = -\delta_2 / \delta_1 \quad (11)$$

Similarly, when a constant stress p is applied along the x_2 direction, that is, $\bar{\sigma}_{11} = 0$, $\bar{\sigma}_{22} = p$, $\bar{\sigma}_{12} = 0$, the equilibrium relationship of the unit cell can be written as follows:

$$\begin{aligned} \left[\int_{-L}^L \sigma_{11}^{(1)}(L, x_2) dx_2 \right] \delta_2 + \left[\int_{-L}^L \sigma_{11}^{(2)}(L, x_2) dx_2 \right] \delta_1 &= 0 \\ \left[\int_{-L}^L \sigma_{22}^{(1)}(x_1, L) dx_1 \right] \delta_2 + \left[\int_{-L}^L \sigma_{22}^{(2)}(x_1, L) dx_1 \right] \delta_1 &= 2Lp \end{aligned} \quad (12)$$

from which, one can get δ_1 and δ_2 . Then the average strains can be given by:

$$\bar{\varepsilon}_{11} = \delta_1 / L, \quad \bar{\varepsilon}_{22} = \delta_2 / L, \quad \bar{\gamma}_{12} = 0 \quad (13)$$

Thus, using the constitutive relation (1), one can determine the effective Young's modulus and Poisson's ratio of the composite by:

$$E_2 = \bar{\sigma}_{22} / \bar{\varepsilon}_{22} = pL / \delta_2, \quad \nu_{21} = -\bar{\varepsilon}_{11} / \bar{\varepsilon}_{22} = -\delta_1 / \delta_2 \quad (14)$$

In-plane shear

For the shear case shown in Figure 2(b), δ_3 and δ_4 are constant displacement constraints to be determined. In the same way, the equilibrium relationship of the unit cell subject to a uniform shear stress p can be written as

$$\begin{aligned} \left[\int_{-L}^L \sigma_{12}^{(3)}(x_1, L) dx_1 \right] \delta_4 + \left[\int_{-L}^L \sigma_{12}^{(4)}(x_1, L) dx_1 \right] \delta_3 &= 2Lp \\ \left[\int_{-L}^L \sigma_{12}^{(3)}(L, x_2) dx_2 \right] \delta_4 + \left[\int_{-L}^L \sigma_{12}^{(4)}(L, x_2) dx_2 \right] \delta_3 &= 2Lp \end{aligned} \quad (15)$$

where $\sigma_{12}^{(3)}$ and $\sigma_{12}^{(4)}$ are shear stresses in the submodels, as described in [8, 11, 22]. Solving Equation (1) yields the unknown δ_1 and δ_2 , and then we have:

$$\bar{\varepsilon}_{11} = 0, \quad \bar{\varepsilon}_{22} = 0, \quad \bar{\gamma}_{12} = (\delta_3 + \delta_4) / L \quad (16)$$

Subsequently, with the shear stress condition $\bar{\sigma}_{11} = 0$, $\bar{\sigma}_{22} = 0$, $\bar{\sigma}_{12} = p$, we finally have

$$G_{12} = \bar{\sigma}_{12} / \bar{\gamma}_{12} = pL / (\delta_3 + \delta_4) \quad (17)$$

3. NUMERICAL RESULTS

To comparison the results from the two different computational models, the following three cases are considered: (a) the centered single circular or square fiber in the unit cell; (b) the circular fiber cluster in the unit cell. The first two cases represent the regular periodic square pattern of fibers in the matrix, while the third case represents the periodically clustered distribution of fibers in the matrix in square pattern (see Figure 3). Moreover, for both the circular fiber and the square fiber, the composite consisting of repeated unit cells can be simplified as isotropic medium, due to the the geometrical symmetry of them. For such case, only three effective elastic parameters of composite need to be determined, $E^c = E_1 = E_2$, $\nu^c = \nu_{12} = \nu_{21}$ and $G^c = G_{12}$. During the computation, the elastic properties of fiber and matrix are [12]

$$E_f = 84\text{GPa}, \nu_f = 0.22, E_m = 4\text{GPa}, \nu_m = 0.34 \quad (18)$$

Besides, various fiber volume fractions covering low fraction to high fraction are studied in this section. For the cases of single circular and square fibers, the value of fiber volume fraction is been set to change from 10 to 70%. For the periodic cluster of circular fibers, the maximum value of the fiber volume fraction is taken to be 50%.

The unit cell is discretized by two-dimensional plane stress linear quadrilateral finite elements implemented in ABAQUS 6.13. In order to achieve accurate and convergent results, a relatively high mesh density is employed so that the maximum relative difference in the predicted Young's modulus between two different meshing schemes is less than a specified tolerance, i.e. 0.1%. Here, the element size is set as one-fiftieth of the side length of the unit cell to satisfy such requirement. Moreover, the side length of the unit cell is 1 for simplicity and the fiber's radius can be evaluated by the given fiber volume fraction.

3. 1. Verification To validate the computational models, the doubly periodic circular hole is first analyzed, which has reference solutions from the BEM [11]. The hole can be viewed as a special inclusion with zero elastic modulus, and the matrix is assumed to have Young's modulus 1 and Poisson's ratio 0.3. During the computation, the hole volume fraction to the unit cell is assumed to change from 0.785 to 38.485%, which covers low and medium contents. Table 1 summarized the numerical results from the free boundary model, the straight-edge model and the BEM, and one can find that there is an excellent agreement between them, especially for the low hole volume contents.

Moreover, the results in Table 1 approximately satisfy the relationship $G^c = E^c / 2(1 + \nu^c)$.

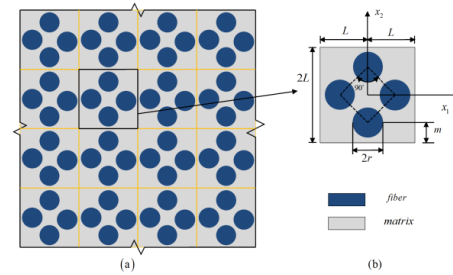


Figure 3. Schematic diagram of composite with periodically clustered fibers in the matrix

TABLE 1. Comparison of results for the case of hole

	V_f	0.785%	7.069%	19.635%	38.485%
E^c	BEM	0.9770	0.8244	0.6168	0.4069
	Free	0.9770	0.8171	0.5916	0.3650
	Straight	0.9771	0.8244	0.6160	0.4062
ν^c	BEM	0.3006	0.2975	0.2665	0.1974
	Free	0.3008	0.3082	0.3234	0.3679
	Straight	0.3007	0.2974	0.2668	0.1969
G^c	BEM	0.3754	0.3045	0.1856	0.0725
	Free	0.3755	0.3072	0.1976	0.0859
	Straight	0.3754	0.3043	0.1856	0.0722

All the three approaches give decreased Young's and shear modulus when the size of hole increases, as expected. However, it is observed that the free boundary model gives higher Poisson's ratio. This can be explained by the unloaded less-constrained opposite edges in the free boundary model, which practically affects the displacement and strain along the perpendicular direction to the tensile direction. More illustrations on such phenomenon can be found in the following tests.

3. 2. Single Fiber For the case of single centered circular fiber in the unit cell, the numerical results obtained by the two different models are plotted in Figures 4-6. It is found that both the Young's modulus and the shear modulus of the composites increase nonlinearly with the increase of fiber volume fraction, however, the Poisson's ratio decreases when the fiber volume fraction becomes larger. Due to the reinforcement of fiber, the Young's modulus of composite is apparently larger than that of matrix, as expected. Also, it is found from Figure 4 that both the free boundary model and the straight-edge model produce similar values of Young's modulus. Additionally, it is seen from Figure 5 that there is significant discrepancy between results of Poisson's ratio from the free-boundary model and the straight-

edge model, and such discrepancy becomes bigger with the increase of fiber volume fraction. The straight-edge model can give smaller prediction of Poisson's ratio than the free boundary model. The main reason is that the free boundary conditions applied on the opposite upper and bottom edges of the unit cell cause the large discrepancy of the prediction of transverse displacement u_2 , which finally affects the average strain component $\bar{\epsilon}_{22}$. Besides, the shear modulus of composite is also shown significant difference, as displayed in Figure 6. Also, the single square fiber is investigated in this study and the simialr trends can be observed.

3.3. Periodically Clustered Circular Fibers Next, the clustered fibers in the matrix is considered. It is assumed that the fiber volume fraction changes from 10 to 50%. Results in Figures 7-9 indicate that the straight-edge model produces higher Young's modulus than the free boundary model again, although the difference of results from them is slight.

Meanwhile, it produces significantly lower Poisson's ratio and shear modulus than the free boundary model, as indicated in Figure 8. Typically, for the free boundary model, the resulted Poisson's ratio is obviously bigger than that of the matrix material.

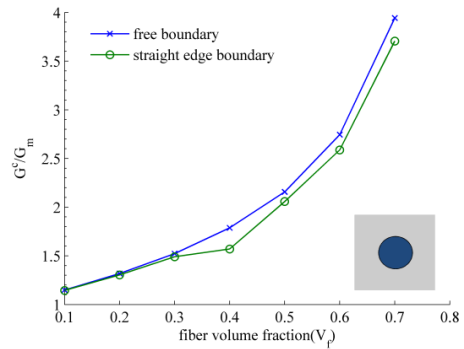


Figure 6. Variation of effective shear modulus for the centered single circular fiber

This can be attributed to the stronger oscillation of displacement solutions along the upper and bottom edges of the unit cell, due to the stronger interaction of fiber cluster and the boundary edges. Therefore, the average strain $\bar{\epsilon}_{22}$ required for evaluating the effective Poisson's ratio of composite may show obvious instability when the fiber volume fraction changes.

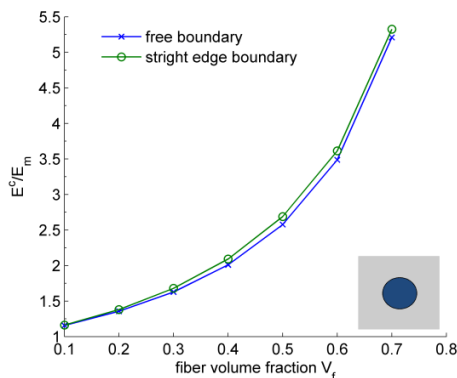


Figure 4. Variation of effective Young's modulus for the centered single circular fiber

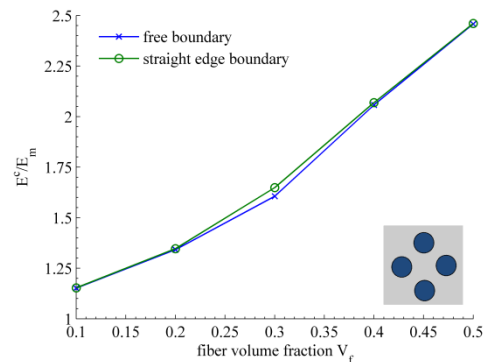


Figure 7. Variation of effective Young's modulus for the periodically clustered circular fibers

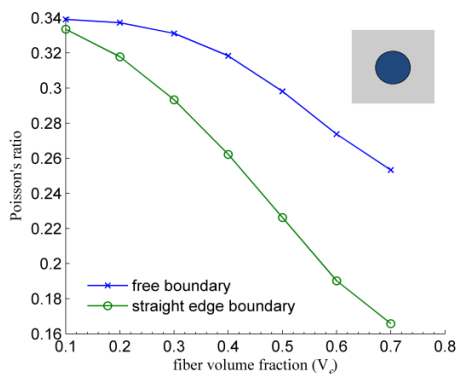


Figure 5. Variation of effective Poisson's ratio for the centered single circular fiber

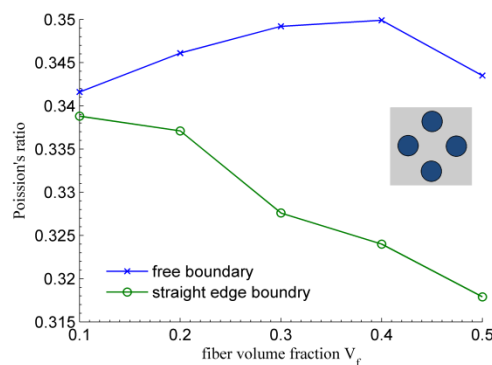


Figure 8. Variation of effective Poisson's ratio for the periodically clustered circular fibers

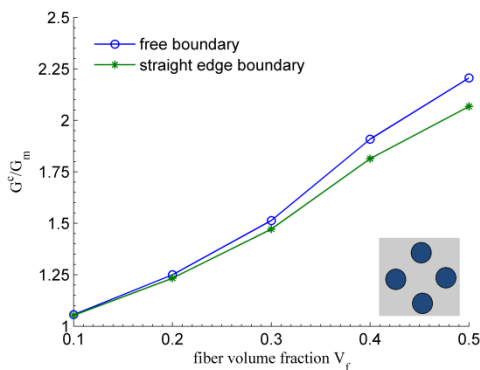


Figure 9. Variation of effective shear modulus for the periodically clustered circular fibers

4. CONCLUSIONS

In this study, the two different models characterizing the transverse elastic properties of unidirectional fiber reinforced composites are compared by considering three tests including the unit cells embedded with centered single circular and square fibers and the centered circular fiber cluster, respectively. It is found that: (1) Both the two models can give increasing Young's modulus as the fiber volume fraction increases. However, the straight-edge model can produce slightly higher values than the free boundary model. (2) The straight-edge model can give lower effective Poisson's ratio than the free boundary model for any fiber volume ratio, and the difference becomes bigger for larger fiber volume fraction. The main reason is that the free boundary conditions applied on the unloaded opposite upper and bottom edges of the unit cell affects the accuracy of the transverse displacement. Applying periodic straight-edge constraints can prevent such over-constrained conditions in the numerical model. (3) Both the two models can give decreasing effective shear modulus of composite when the fiber volume fraction increases, and the results from the straight-edge model is always lower than that from the free boundary model.

5. REFERENCES

1. Kaw, A.K., "Mechanics of composite materials, Boston, CRC Press, Vol. 51, (2006).
2. Jhanji, K.P., Kumar, R.A. and Likhith, P., "Influence of circular and square cut-outs on fiber glass/epoxy composite laminate under tensile loading", *International Journal of Engineering*, Vol. 31, No. 1, (2018), 104-109.
3. Prasanth, I.S.N.V.R., Ravishankar, D.V. and Hussain, M.M., "Analysis of milling process parameters and their influence on glass fiber reinforced polymer composites", *International Journal of Engineering*, Vol. 30, No. 7, (2017), 1074-1080.
4. Priya Jhanji, K., Amit Kumar, R. and Likhith, P., "Influence of circular and square cut-outs on fiber glass/epoxy composite laminate under tensile loading", *International Journal of Engineering*, Vol. 31, No. 1, (2018), 104-109.
5. Khamedi, R., Ahmadi, I., Hashemi, M. and Ahmaditabar, K., "Stiffness prediction of beech wood flour polypropylene composite by using proper fiber orientation distribution function", *International Journal of Engineering*, Vol. 30, No. 4, (2017), 582-590.
6. Ko, Y.F. and Ju, J.W., "New higher-order bounds on effective transverse elastic moduli of three-phase fiber-reinforced composites with randomly located and interacting aligned circular fibers", *Acta Mechanica*, Vol. 223, No. 11, (2012), 2437-2458.
7. Kushch, V.I., Shmegeera, S.V., Brondsted, P. and Jr, L.M., "Numerical simulation of progressive debonding in fiber reinforced composite under transverse loading", *International Journal of Engineering Science*, Vol. 49, No. 1, (2011), 17-29.
8. Lei, Y.P., Wang, H. and Qin, Q.H., "Micromechanical properties of unidirectional composites filled with single and clustered shaped fibers", *Science & Engineering of Composite Materials*, Vol. 25, No. 1, (2018), 143-152.
9. Kari, S., Berger, H. and Gabbert, U., "Numerical evaluation of effective material properties of randomly distributed short cylindrical fibre composites", *Computational Materials Science*, Vol. 39, (2007), 198-204.
10. Wang, H., Liu, B., Kang, Y.X. and Qin, Q.H., "Analysing effective thermal conductivity of 2d closed-cell foam based on shrunk voronoi tessellations", *Archives of Mechanics*, Vol. 69, No. 6, (2017), 451-470.
11. Dong, C.Y., "Effective elastic properties of doubly periodic array of inclusions of various shapes by the boundary element method", *International Journal of Solids & Structures*, Vol. 43, No. 25-26, (2006), 7919-7938.
12. Liu, Y.J., Xu, N. and Luo, J.F., "Modeling of interphases in fiber-reinforced composites under transverse loading using the boundary element method", *Journal of Applied Mechanics*, Vol. 67, (2000), 41-49.
13. Qin, Q.H. and Wang, H., "Special elements for composites containing hexagonal and circular fibers", *International Journal of Computational Methods*, Vol. 12, No. 4, (2015), 1540012 (1540017 pages).
14. Wang, H. and Qin, Q.H., "A new special coating/fiber element for analyzing effect of interface on thermal conductivity of composites", *Applied Mathematics and Computation*, Vol. 268, (2015), 311-321.
15. Wang, H., Zhao, X.J. and Wang, J.S., "Interaction analysis of multiple coated fibers in cement composites by special n-sided interphase/fiber elements", *Composites Science and Technology*, Vol. 118, (2015), 117-126.
16. Wang, H., Qin, Q.H. and Xiao, Y., "Special n-sided voronoi fiber/matrix elements for clustering thermal effect in natural-hemp-fiber-filled cement composites", *International Journal of Heat and Mass Transfer*, Vol. 92, (2016), 228-235.
17. Kalamkarov, A.L., Andrianov, I.V. and Danishevskyy, V.V., "Asymptotic homogenization of composite materials and structures", *Applied Mechanics Reviews*, Vol. 62, (2009), 030802.
18. Wang, J.L., Crouch, S.L. and Mogilevskaia, S.G., "Numerical modeling of the elastic behavior of fiber-reinforced composites with inhomogeneous interphases", *Composites Science and Technology*, Vol. 66, (2006), 1-18.
19. Sadowski, T. and Pankowski, B., "Numerical modelling of two-phase ceramic composite response under uniaxial loading", *Composite Structures*, Vol. 143, (2016), 388-394.
20. Chen, Y.Z. and Kang, Y.L., "Two-dimensional elastic analysis of doubly periodic circular holes in infinite plane", *KSME International Journal*, Vol. 16, No. 5, (2002), 655-665.

21. Antunes, F.V., Ferreira, J.A.M. and Capela, C., "Numerical modelling of the young's modulus of syntactic foams", *Finite Elements in Analysis and Design*, Vol. 47, (2011), 78-84.
22. Wang, H., Kang, Y.X., Liu, B. and Qin, Q.H., "Effect of the orientation of hexagonal fibers on the effective elastic properties of unidirectional composites", *Journal of Mechanics*, Vol. 34, No. 3, (2018), 257-267.

Comparison of Two Computational Microstructure Models for Predicting Effective Transverse Elastic Properties of Unidirectional Fiber Reinforced Composites

W. Lin^a, H. Wang^{a,b}, Y. Zhang^a

^a College of Civil Engineering & Architecture, Henan University of Technology, Zhengzhou, China

^b State Key Laboratory of Structural Analysis for Industrial Equipment, Dalian University of Technology, Dalian, China

P A P E R I N F O

چکیده

Paper history:

Received 10 November 2017

Received in revised form 23 December 2017

Accepted 04 January 2018

Keywords:

Fiber-reinforced Composite
Effective Transverse Elastic Properties
Free Boundary
Straight-edge Boundary
Finite Element

مشخصه خواص کامپوزیت‌ها توجه زیادی به مطالعه برنامه‌های کاربردی آن در مهندسی دارد. هدف از این کار مطالعه تفاوت دو مدل ریزساختار محاسباتی است که به طور گسترده‌ای برای تعیین خواص کششی موثر برای کامپوزیت‌های تقویت شده فیبری همسو استفاده می‌شود. اولین مدل مبتنی بر مکانیک کلاسیک مواد مجاز آزادانه تخلیه مرزهای مخالف در سلول واحد است. در حالی که دومین محدودیت‌های خطی را در سلول واحد برای نشان دادن تعاملات سلول‌های اطراف در طی تغییر شکل می‌دهد. این دو روش ابتدا توسط طرح مسئله در سوراخ دایره‌ای تایید شده است. سپس سه ریزپردازنده شامل الیاف دایره‌ای، فیبرهای مربعی و خوشه‌های فیبر دایره‌ای که به صورت دوره‌ای در ماتریس قرار می‌گیرند و سپس با تجزیه و تحلیل عناصر محدود حل می‌شوند، مورد توجه قرار می‌گیرند. مقایسه نتایج عددی نشان داد که دو مدل محاسباتی با و بدون شرایط دوره‌ای می‌تواند پیش‌بینی‌های مختلفی بر خواص موثر کششی کامپوزیت برای هر دو فاکتور حجم کم و زیاد، بخصوص برای نسبت موثر پواسون کامپوزیت ارائه دهد. اعمال محدودیت‌های مستقیم خطی پس از تغییر شکل می‌تواند مانع هرگونه شرایط بیش از حد محدود در مدل عددی شود و نتایج پایدارتری را ارائه دهد.

doi: 10.5829/ije.2018.31.09c.04